

Biosorption of Chromium (II) Ion from Textile Effluent Using Watermelon Shell-Activated Carbon

Chukwu Emmanuel Okam¹, Godfrey Ifeanyi Odo¹, Chinweikpe Kalu Uduma¹, Okolo Bernard¹, Gift Uzunma Ijioma¹

¹ Michael Okpara University of Agriculture, Umudike
PMB 7267, Umuahia Umudike, Abia State, Nigeria

DOI: [10.22178/pos.85-2](https://doi.org/10.22178/pos.85-2)

LCC Subject Category: TN1-997

Received 20.08.2022

Accepted 20.09.2022

Published online 30.09.2022

Corresponding Author:

Chukwu Emmanuel Okam

chukwuokam.e@gmail.com

© 2022 The Authors. This article is licensed under a [Creative Commons Attribution 4.0 License](https://creativecommons.org/licenses/by/4.0/)



Abstract. Watermelon Shell, an agricultural waste, was employed for the adsorptive removal of chromium (II) ion Cr^{2+} from textile effluent. This study analysed the adsorbent's active sites and morphological structures using FT-IR, SEM, XRD, and XRF. The independent variables' effect, contact time, adsorbent dosage, and pH were predicted using Response Surface Methodology (RSM) for chromium adsorption onto Watermelon Shell Activated Carbon (WSAC). The experimental results indicated that NaOH activation effectively improved WSAC's adsorption capacity. The maximum adsorption capacity was 54.53 %, with an adsorbent dosage of 0.6 g/l, pH of 6.0, and agitation time of 40 min. The high correlation coefficient ($R^2=0.978$) between the model and the experimental data showed that the model predicted the removal of Cr^{2+} from textile effluent using Watermelon Shell Activated Carbon efficiently.

Keywords: Activated Carbon; Chromium Adsorption; Heavy Metals; Adsorption; Watermelon Shell; Textile Effluent; Carbonisation.

INTRODUCTION

Wastewater is any water whose quality has been negatively impacted by human activity. Wastewater can originate from domestic, industrial, commercial, or agricultural activities, surface runoff or stormwater, and sewer inflow or infiltration [1]. Significant health hazards are related to using untreated wastewater for domestic purposes, agriculture, etc. The presence of heavy metals in wastewater is one of the most challenging environmental problems due to their toxicity, persistence, and bioaccumulation tendencies [2]. Many industries produce and discharge metal-containing wastes mostly into water bodies. This affects the water's aesthetic quality and increases the concentrations of metals present [3]. These heavy metals commonly include; Cd, Pb, Cu, Fe, Ni, Mn, and Cr. Heavy metal contamination is not a recent problem, but its management and prevention are still of global concern [4]. Textile industries contribute immensely to surface water deterioration and are categorised among the most polluting in all industrial sectors [5]. The dyeing and printing of textiles have a significant

environmental impact since they use a lot of water and generate a lot of highly contaminated wastewater.

The pollutants created by the textile dyeing and printing industries are influenced by the chemicals used in the various dyeing and printing processes. The receiving water thus becomes brackish. Textile dyes are toxic, highly stable and do not degrade quickly, and are not removed by conventional wastewater treatment methods. Due to the environment's non-degradable nature and long-time persistence, the toxic waste often accumulates at a low level, causing a harmful biological effect [6].

In addition, effluent or wastewater from textile production discharged into the water body without proper treatment also seeps through the aquifer and pollutes the underground water in many ways. Besides colour visibility which brings displeasing aesthetics, heavy metal constituents in the effluent also result in adverse environmental impacts on the water body and environment as well as deterioration of human health [7].

During operations, they also produce heat from effluents released, increased pH, and water saturation with dyes, defoamers, bleaches, detergents, optical brighteners, and equalisers. Due to these, pollutants from the textile production sector are being released into the environment at various stages of operation. Heavy metals, notably lead (Pb), Chromium (Cr), cadmium (Cd), and copper (Cu), are used widely for the colour pigment production of textile dyes. Such heavy metals can exist naturally in the structures of textiles or penetrate textile fibres during the show, the dyeing process, or through protective agents used during storage. These heavy metals, which have been transferred to the environment, are highly toxic and can bioaccumulate in the human body, aquatic life, and natural water bodies and possibly be trapped in the soil [8].

Lead (II) ion has been reported to be responsible for intellectual disabilities in children and causes about 143,000 deaths annually in developing countries [9]. Young children are vulnerable to lead exposure because it affects the development of the brain and nervous system [10]. It can also result in miscarriage, low birth weight, stillbirth, premature birth in pregnant women, kidney damage, and high blood pressure in adults [11]. Ingestion of lead-contaminated water has been implicated as a significant route of lead toxicity.

Several techniques have been designed for heavy metals removal from aqueous solutions, including ion exchange, chemical precipitation/co-precipitation, filtration, coagulation, membrane technologies, and commercial activated carbon [12]. The significant drawbacks to these methods lie in the cost involved, the efficiency of the processes, and the disposal of wastes generated [13]. These disadvantages have made researchers seek alternative techniques for heavy metal remediation.

Hazardous metals can reportedly be removed from industrial effluents by adsorbing using naturally occurring elements. This method uses dead waste biomass, microorganisms, and other naturally plentiful plant components as raw materials [14]. The sorption capacity of some biosorbents is high due to the presence of adequate functional groups that sequester metals from aqueous solutions [13]. This method's application is affordable, sustainable, and readily available. These bio-based materials have demonstrated a propensity to eliminate metals at trace levels, thereby addressing some of the major draw-

backs of conventional techniques [15]. Several adsorbents from plant origin have been used and modified for heavy metal removal from wastewater and aqueous solution, which include: maize tassels, coffee beans, coconut shells, peanut shells, *Annona squamosa* shells, rice husks, rice bran, orange peels, sunflower stem, groundnut shells and avocado seed [16, 17]. This study presents Watermelon Shell Activated Carbon as a potential, environmentally friendly, and low-cost adsorbent for the adsorption of metals from textile wastewater samples. In Watermelon, the red flesh inside is sweet, edible, and used for juices and salads, but the outer shell is considered waste and has no commercial value [18].

The watermelon shell consists of pectin, citrulline, cellulose, proteins, and carotenoids [19]. The polymers are rich in functional groups like hydroxyl (cellulose) and carboxylic (pectin). They can easily bind metal ions by changing their hydrogen ions for metal ions or giving an electron pair to form complexes with the metal ions [20]. The idea behind the adsorption of heavy metals using watermelon shells is to treat waste with waste and become even more effective because these agricultural by-products are easily accessible and frequently cause issues with garbage disposal.

Because they are waste items, they can be found for little to no money. Also, this makes treating wastewater with agricultural by-product adsorbents more economical than using conventional adsorbents like activated carbon. This research conducted characterisation and optimisation studies for textile effluent and watermelon shells.

MATERIALS AND METHODS

Effluent Collection. The raw effluent was collected from Rosie's textile Company in Aba, Abia state, in a sterile 20 litres gallon from its point of discharge to the environment. It was stored at room temperature without further purification [21].

Collection of Adsorbent. Watermelon shells (WS) were obtained from different fruit-selling sources in Umuahia, Abia state, and washed with clean water. The watermelon shells were cut into small pieces and dried in sunlight for 14 days to remove all moisture content present. The dried watermelon shells were stored in an air-tight container.

Carbonisation. Carbonisation (1500 grams of washed, cut, and dried watermelon shells) was carried out in a muffle furnace (KGYV BUDAPEST KCC086/50-120.3 phases) at about 500-700 °C for two hours and was held at this temperature for 60 min, after which the charred products were allowed to cool to room temperature.

Preparation of 60% Alkaline (NaOH) Used for Activation. 40 g of NaOH pellet was carefully weighed using an electronic balance (YP502N) and dissolved in 1000 ml of distilled water using a measuring cylinder. 400 ml of the dissolved NaOH was removed and stored in an air-tight container. The remaining 600 ml of the dissolved NaOH was diluted up to 1000 ml of NaOH solution with distilled water. This gave the required 60% solution of NaOH.

Preparation of Activated Carbon. The charred material obtained from watermelon shell carbonisation was crushed into smaller sizes to pass through a 3 mm sieve and retained in a 1.5 mm sieve. 302 g of the sample was weighed using an electronic balance (YP502N) and impregnated in the alkaline solution (60 % NaOH) in a beaker. The mixture was stirred with a glass rod to mix well and left for 24 hours for proper impregnation. At the end of the 24 hours, the mixture was washed with distilled water until the tested pH of the water washed out became near neutral [22]. The sample was dried in an oven for 1 hour at 105 °C and stored in an air-tight container.

Textile Effluent Characterization. The effluent was analysed for the presence of heavy metals (nickel, vanadium, zinc, lead, calcium, manganese, chromium, sodium, iron, and copper) by digesting 100 ml of the effluent using a 10 ml triple acid mixture (5:1:1 - HNO₃:HClO₄:H₂SO₄) in a 250 ml conical flask. The sample was properly covered with aluminium foil to avoid spillage and heated on a hot plate until the solution was reduced to 10 ml. After that, it was allowed to cool and make up to a mark by topping with distilled water before it was filtered into a 50 ml standard flask ready for further analysis. The concentrations of the heavy metals in the wastewater were determined using Atomic Absorption Spectrometer (AA-7000). The result is given in Table 1.

Batch Adsorption. 100 ml of the textile effluent was transferred to 250 cm³ Erlenmeyer flasks after the initial pH of the sample's effluent had been determined. 0.2 g of Watermelon Shell Activated Carbon (WSAC) was weighed and added to the effluent. The solution was agitated for 10 min using a speed-adjusting multipurpose vibrator

(HY-2) at 100 rpm. Adsorbent dose, contact time, pH, and beginning concentration were among the adsorption parameters whose effects were investigated. Using 0.1 M HCl and 0.1 M NaOH as adjustments, the impact of pH on adsorption was assessed by altering the pH from 2–10. The contact period was changed from 10 to 70 min, and the adsorbent dosage was changed from 0.2 to 1 gram per litre to determine its impact. The solid phase was separated for each parameter study using filter paper, and the remaining metal concentration in the supernatant was assessed using an atomic absorption spectrophotometer (MODEL: AA-700).

Adsorbent Characterization

Proximate Analysis. Proximate analysis was carried out on the WSAC to determine the moisture content, ash content, fat content, crude protein, crude fibre, and carbohydrate using AOAC 2005 method. The result is presented in Figure 5.

FTIR Analysis. The sample was analysed using FTIR technology of the mark SPECTRUM ONE FTIR combined with software (Perkin Elmer Instruments version 3.02.01) to study the spectra. 0.5 g of activated carbon was added to the spectrophotometer for sample analysis. For sample analysis, 0.5 g of activated carbon was introduced into the spectrophotometer for analysis. The wave number varied between 4000 and 350 cm⁻¹.

X-ray Fluorescence (XRF) Analysis. This was performed to know the chemical compositions of the minerals in the adsorbent. X-ray fluorescence analysis of the adsorbent was done using model PW 2400/0.

X-ray diffraction (XRD) Analysis. X-ray (XRD-6000 SHIMADZU Japan) was used to scan the activated carbon used in this work. This was done at 2θ value between 100 and 800 at a scan rate of 2 degrees per minute.

Scanning Electron Microscope Analysis. A scanning electron microscope (SEM) was used to determine the morphological structure of the activated carbon before and after adsorption.

Adsorption Kinetics and Isotherms

Kinetics of Adsorption. The kinetics of adsorption was examined by examining the adsorptive uptake of heavy metals from wastewater at various time intervals. The pseudo-first-order and pseudo-second-order model equations were used to simulate the rate at which heavy metals bind to the created activated carbon.

The linearity of each model was plotted. As a result, in this work, the model parameters were calculated utilising the data produced by the experiments performed and considering the linearised forms of the pseudo-first-order and pseudo-second-order reaction models, respectively.

$$\log(q_e - q_t) = \log(q_e) - \frac{k_1}{2.303} t \quad (1)$$

$$\left(\frac{t}{q_t}\right) = \frac{1}{k_2 q_e^2} + \frac{1}{q_e} (t) \quad (2)$$

Adsorption Isotherm. With the aid of the data generated from the adsorption studies of this work, the parameters contained in the Langmuir adsorption isotherm were estimated.

$$q_e = \frac{q_m K_L C_e}{1 + K_L C_e} \quad (3)$$

The linearisation of equation (3) leads to the following form:

$$\frac{1}{q_e} = \frac{1}{q_m K_L C_e} + \frac{1}{q_m} \quad (4)$$

Experimental Design. The design and analysis of variables were evaluated using Design-Expert V6.0.8. Response surface methodology (RSM) is a statistical method that uses quantitative data from appropriate experiments to determine regression model equations and operating conditions. A standard RSM design called Box-Behnken Design (BBD) was applied in this work to study the variables for removing chromium from an aqueous solution using a batch process. BBD was used as an experimental design model for three variables (adsorbent dosage, pH of solution, and agitation time), each with three levels (the minimum, medium and maximum). Seventeen experiments [22] are needed to conduct and determine ten coefficients of the second-order polynomial equation [23]. In the experimental design model, adsorbent dosage (0.2-1.0 g/l), pH (2-10), and agitation time (10-70 min) were taken as input variables. The percentage removal of chromium was taken as the response of the system. Three factors were studied, and their low and high levels are given in Table 1.

Table 1 – Coded and actual values of variables of the experimental design

Factor		Coded levels of variables		
		-1	0	1
Adsorbent dosage	A	0.2	0.6	1.0
pH	B	2	6	10
Agitation time	C	10	40	70

RESULTS AND DISCUSSION

Textile effluent and proximate analysis. The result of the characterisation of the textile effluent before adsorption (Table 2), conducted using an Atomic Absorption Spectrometer (AA-7000), indicated the presence of heavy metals.

Table 2 – Characterisation of textile effluent before adsorption

Metals	Concentration
Calcium, ppm	3.3333
Chromium, ppm	1.3333
COD	170.4
Sulphate	18.24
Manganese, ppm	0.0324
Sodium, ppm	1.4883
Vanadium, ppm	2.0000
Zinc, ppm	0.0693
Nickel, ppm	0.2051
TOC	8.78
Ph	6.41
BOD, m/l	51.2
Chloride	252.76
Nitrate	16.08
Phosphate	1.5
TDS	758.87

After the proximate composition characterisation of the activated carbon (Table 3), the result stated fixed carbon content of 80.37% at a 25.7% yield.

Table 3 – Proximate composition analysis results of WSAC

Parameter	Result
Moisture content (%)	24.50
Ash (%)	17.50
Volatile matter (%)	14.25
Surface area (m ² /g)	847.43
Fixed carbon (%)	80.37
Bulk density (gcm ³)	0.4
Iodine number	724.64
Yield (%)	25.7

FTIR Analysis. The FT-IR spectra of unloaded WSAC (Fig. 1a) indicated a band at 3395.79 cm⁻¹ due to the O–H stretching of water. The band observed at 2935.76 cm⁻¹ corresponded to methylene asymmetric, H–H stretching. The band at 1592.29 cm⁻¹ indicated the presence of pyridine, C=N stretching, while the band at 1402.3 cm⁻¹ was ascribed to azo compound, N=N stretching. Finally, the band at 1084.03 cm⁻¹ was found to be due to aliphatic C–N stretching, while the band at 683.79 cm⁻¹ was due to P=S stretching. After the adsorption of the metal ions present in the effluent by the activated carbon, the FT-IR spectra (Figure 1b) showed shifts in some of the bands and new bands. For instance, the bands at 406.03, 683.79, 1084.03, 1403, 1592.29, 2935.76, and, 3395.79 cm⁻¹ were shifted to 408.92, 786.02, 1099.46, 1399.4, 1599.04, 2934.79 and 3400.62 cm⁻¹, respectively. The shifts in the bands confirmed the participation of the functional groups in the adsorption of the metal ions of the effluent onto the developed activated watermelon shell carbon.

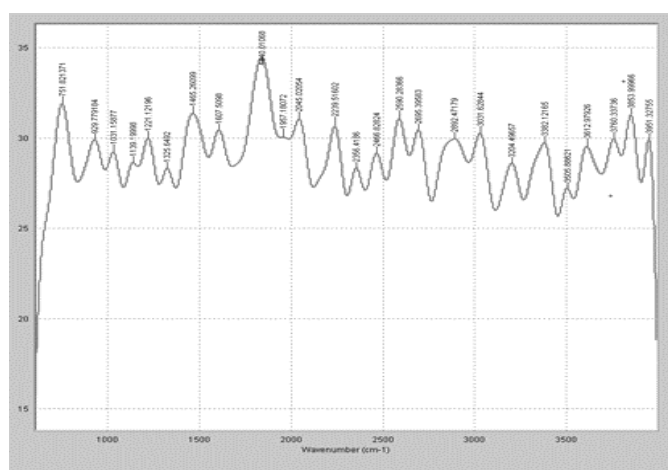


Figure 1a – FT-IR spectrum for WSAC before adsorption

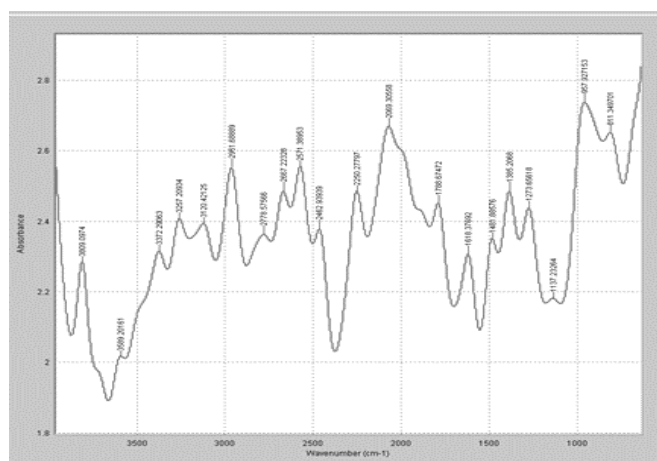


Figure 1b – FT-IR spectrum for WSAC after adsorption

XRF Analysis. From the result of the XRF before and after the biosorption (Table 4), the concentration of silica oxide (SiO₂) was 83.70%, the highest among the chemical composition. It shows that the loading of Cr was 24.40% after biosorption.

Table 4 – XRF chemical analysis of the WSAC samples

Formula	Concentration before adsorption (%)	Concentration after adsorption (%)
CO ₂	0.10	0.1
SiO ₂	83.70	1.18
SO ₃	8.32	0.93
CaO	2.18	0.15
Al ₂ O ₃	1.61	0.26
Fe ₂ O ₃	1.00	1.34
P ₂ O ₅	0.99	0.003
K ₂ O	0.87	0.20
Cl	0.82	0.11
MoO ₃	0.30	0.05
Cr	ND	24.40

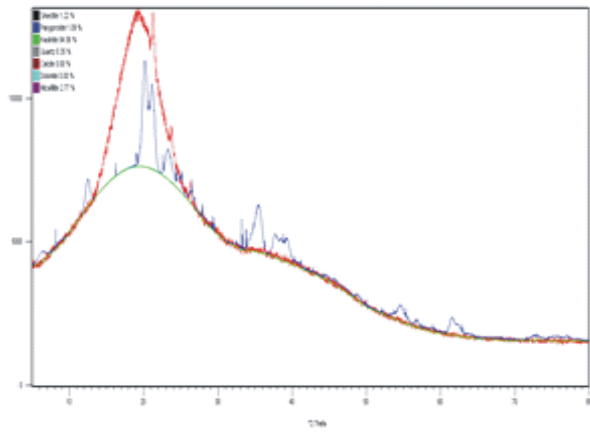
X-ray diffraction analysis (XRD). The WSAC has an utterly amorphous structure which is expected for organic materials. Sharp peaks are absent, revealing a predominantly amorphous structure, an advantageous property of a well-defined porous adsorbent [24]. The X-ray diffraction pattern of the samples in Figure 2 shows the presence of mica/illites, kaolinite, and quartz.

The reflection associated with mica/illites is characterised by reflection located at 2θ=17° and 25° and kaolinite at 2θ=20° and 21° for WSAC before adsorption. For WSAC after adsorption, mica/illites were located at 15°, 18°, and 24°, and kaolinite at 20° and 22°.

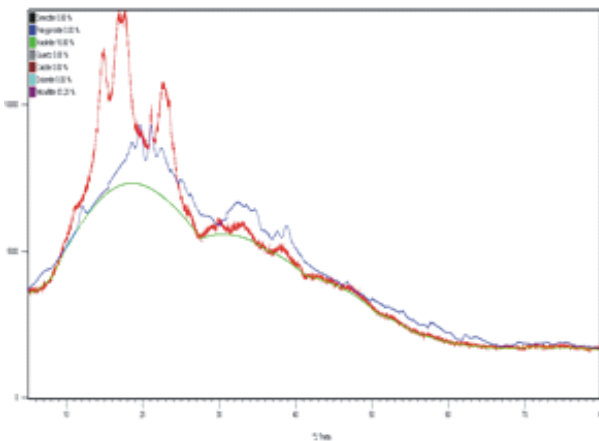
Table 5 – X-ray diffraction results for the adsorbent

Phase	Before	After
Smectite	0.15	0.00
Palygorskite	0.00	0.82
Kaolinite	0.00	2.87
Quartz	16.90	15.74
Calcite	0.85	0.61
Dolomite	0.57	2.37
Mica/illite	81.54	77.59

Other reflections are attributed to the activated carbon, like smectite, palygorskite, calcite, and dolomite. Other researchers also reported this outcome [27].



a)



b)

Figure 2 – X-ray diffraction pattern of WSAC before (a) and after (b) adsorption

Morphology and Textural Examination of the Adsorbent. From the SEM results (Figure 3a), the watermelon shell gave a porous surface texture, enabling metal ions' adsorption onto the surface. Besides, it also shows that the surface morphology of the watermelon shell consisted of two kinds of colour tones: lighter and darker [26].

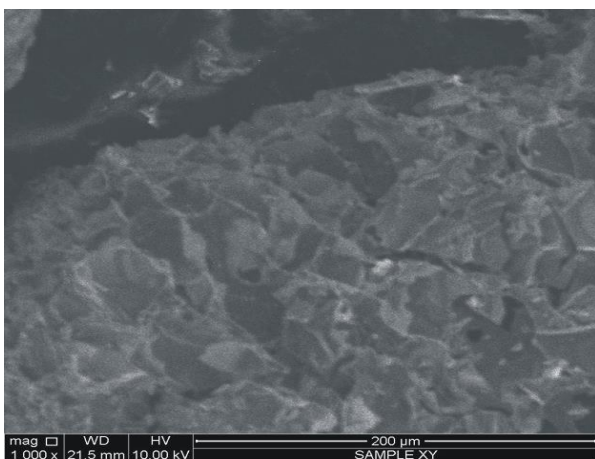


Figure 3a – SEM image of WSAC before adsorption 1000 magnification

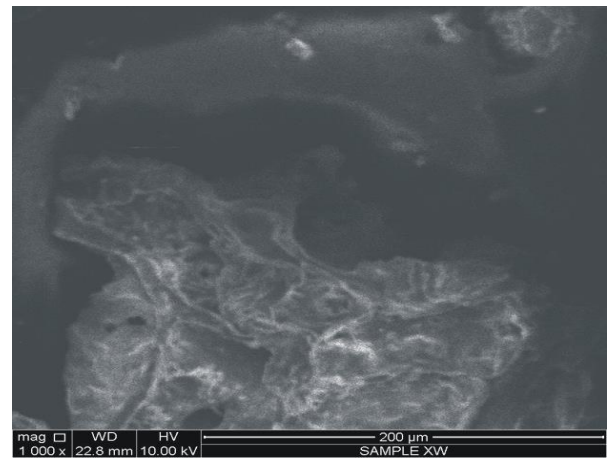


Figure 3b – SEM image of WSAC after adsorption at 1000 magnification

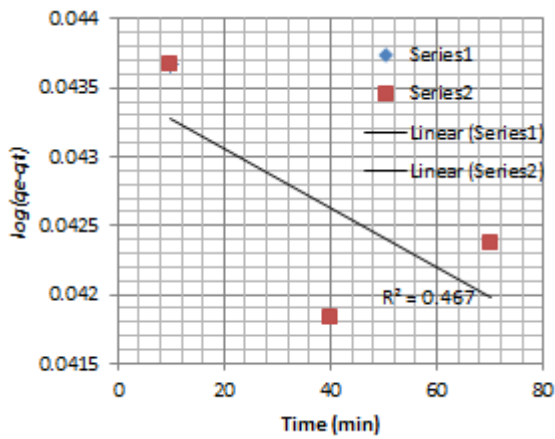
The lighter shades represented the inorganic component, while the darker shades were organic components. From the spectrum of the watermelon shell (Figure 3a), Si was observed. After the biosorption of Cr using a watermelon shell, the morphology underwent a physical change. Lump-like deposits or shiny particles were formed (Figure 3b).

Adsorption Kinetics. The pseudo-first-order and pseudo-second-order model equations were fitted to model the kinetics of heavy metal adsorption onto the produced activated carbon. When plotted, the linearity of each model was used to determine how suitable each model was for the adsorption. As a result, the model parameters were calculated in this study utilising the data produced by the experiments conducted and taking into account the linearised versions of the pseudo-first-order and pseudo-second-order reaction models provided in Equations (5) and (6), respectively.

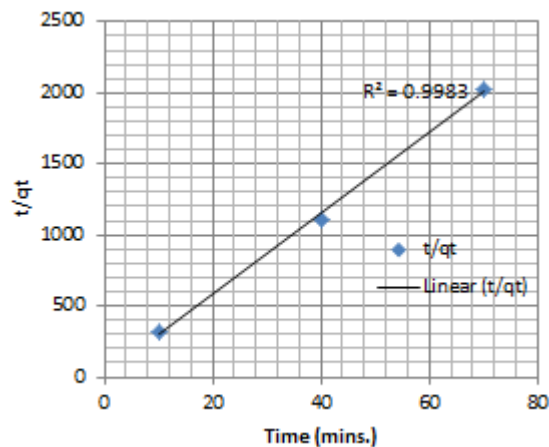
$$\log(q_e - q_t) = \log(q_e) - \frac{k_1}{2.303} t \tag{5}$$

$$\left(\frac{t}{q_t}\right) = \frac{1}{k_2 q_e^2} + \frac{1}{q_e} (t) \tag{6}$$

It was found that the pseudo-second-order model fitted better than the pseudo-first-order model for the removal of Cr²⁺ by Watermelon with R²=0.9983 (Figure 4).



Pseudo-first-order kinetic



Pseudo-second-order kinetic

Figure 4 –Pseudo first and Second-Order plot for Cr²⁺ Removal by WSAC

Adsorption isotherm. The results obtained from chromium adsorption using 100 ml textile wastewater and 0.6 g WSAC at 40 min agitation time and pH of 6 (Figure 5) gave an R² value of 0.9993.

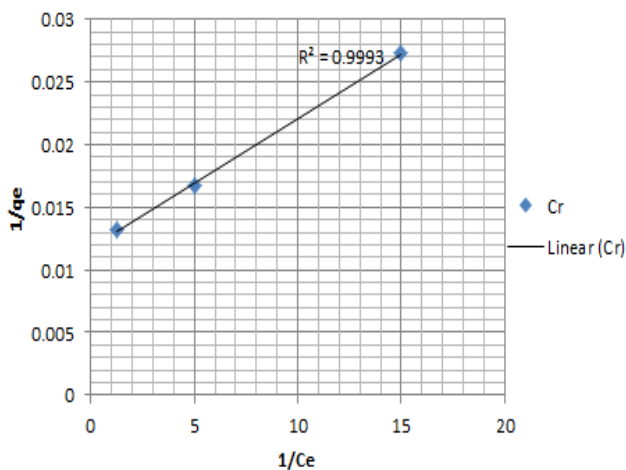


Figure 5 – Langmuir adsorption isotherm for adsorption of Cr²⁺ on WSAC

Statistical Optimization of Removal of Chromium Using WSAC. A BBD with a total of 17 experiments was employed for RSM. Table 6 reports the experimental and predicted values of the adsorption capacity of WSAC.

Table 6 – Experimental design and results for the copper removal

Run	Coded values			Actual values			Removal	
	A	B	C	A	B	C	Observed	Predicted
1	1	0	-1	1	6	10	50.66	51.13
2	1	1	0	1	10	40	52.07	52.16
3	0	0	0	0.6	6	40	37.82	37.72
4	0	1	-1	0.6	10	10	54.53	54.06
5	0	-1	1	0.6	2	70	35.08	34.01
6	-1	0	1	0.2	2	70	50.75	50.05
7	1	0	1	1	6	70	46.13	46.83
8	0	-1	-1	0.6	2	10	47.09	48.16
9	-1	-1	0	0.2	2	40	33.65	34.25
10	0	0	0	0.6	6	40	33.51	34.67
11	0	0	0	0.6	6	40	47.05	45.89
12	-1	0	-1	0.2	2	10	34.56	33.96
13	0	0	0	0.6	6	40	44.04	44.55
14	0	1	1	0.6	10	70	46.00	44.55
15	-1	1	0	0.2	10	40	42.34	44.55
16	0	0	0	0.6	6	40	44.56	44.55
17	1	-1	0	1	2	40	45.79	44.55

The coefficient of determination (R²) presents the quality of the polynomial model [28]. The predicted R² considers all effects, and the adjusted R² considers only square effects and interaction effects between two input variables. This study's predicted R² and adjusted R² were 0.8225 and 0.9867, respectively, indicating that the model could not explain only 17.75 % of total variations. "Adeq Precision" measures the signal-to-noise ratio, and a ratio greater than four is desirable. The balance was 17.36 in this study, indicating an adequate signal. Therefore, the RSM model could be used to navigate the design space [12].

The experimental and predicted values closely match the R² value of 0.978 (Figure 6).

So, the high correlation coefficient (R²=0.978) between the model and the experimental data showed that the model could efficiently predict the removal of Cr²⁺ from textile effluent using WSAC. This methodology could be successfully employed to study the importance of the test variables' individual, cumulative, and interactive effects in biosorption.

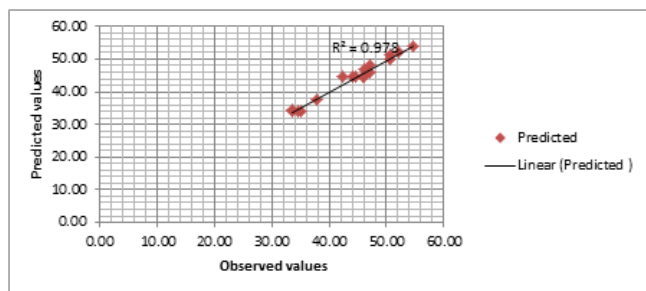


Figure 6 – Parity plot showing the distribution of experimental vs predicted values of percentage removal of Cr^{2+}

The optimum values of adsorbent dosage, pH and agitation time from BBD were found to be 0.6 g/l, six and 40 min, respectively. The maximum predicted removal of Cr^{2+} was found to be 54.06%.

The developed model equation in terms of coded factors is as follows:

$$\text{REMOVAL} = + 44.55 + 4.34*A - 2.88*B + 2.73*C + 5.89*A^2 - 1.67*B^2 - 5.68*C^2 + 3.83*A*B - 3.68*A*C - 3.09*B*C$$

where the response was the removal of chromium from textile effluent, A was the coded value of dosage of adsorbent, B was the coded value of pH of the solution, and C was agitation time.

The coefficients with one factor represent the effect on the particular factor, while the coefficients with two elements represent the interaction between the two factors. The positive sign in the equation indicates a synergistic effect, whereas the negative sign indicates an antagonistic effect.

From the analysis of variance (ANOVA) for the response surface quadratic model (Table 7), the model F-value of 34.50 implied that the RSM model is significant.

Table 7 – Analysis of variance (ANOVA) for the removal of chromium (%) with WSAC

Source	Sum of Squares	DF	Mean Squares	F-Values	P Prob > F	Comment
Model	707.13	9	78.57	34.5	< 0.0001	Significant
A	150.89	1	150.89	66.25	< 0.0001	Significant
B	66.18	1	66.18	29.05	0.001	Significant
C	59.65	1	59.65	26.19	0.0014	Significant
A ²	146.31	1	146.31	64.24	< 0.0001	Significant
B ²	11.78	1	11.78	5.17	0.0571	
C ²	135.81	1	135.81	59.63	0.0001	Significant
AB	58.55	1	58.55	25.71	0.0014	Significant
AC	54.06	1	54.06	23.73	0.0018	Significant
BC	38.11	1	38.11	16.73	0.0046	Significant
Residual	15.94	7	2.28			
Lack of Fit	7.16	3	2.39	1.09	0.4501	Not significant
Pure Error	8.78	4	2.2			
Cor Total	723.07	16				
R ²	0.978					
Adj. R ²	0.9496					
Pred. R ²	0.8225					
Adeq. Precision	17.364					
Std. Dev.	1.51					
C.V.	3.44					

The p values are used to check the significance of each of the coefficients. The p values less than 0.05 indicate that the RSM model terms are significant. In this study, A, B, C, A², C², AB, AC, BC are practical model terms. A, B, C² (p<0.0001) were the essential terms for the Chromium adsorption capacity.

The coefficient of variation (the ratio of the standard error of estimate to the mean value stated as a percentage) and F-value tests have

also been carried out to assess the model's suitability.

The F-distribution is a probability distribution that compares variances by looking at their ratio. If they are equal, then the F-value would equal one. The balance of the model means square (MS) to the relevant error means the F-value represents square in the ANOVA table.

The F-value increases along with the ratio, increasing the likelihood that the model's mean square contribution will be much more significant than the error mean square. For R^2 closer to unity, the better the estimated regression equation fits the response data. The closeness of R^2 and Adj. R^2 signified that the significant terms and effects are genuinely substantial. Hence the model worked well. The agreement of Adj. R^2 and Pred. R^2 (i.e., a difference of < 0.2) authenticated that the model truly fits.

Effect of pH and dosage. pH and adsorbent dosage is the essential process parameters for assessing the removal capacity of a biosorbent. Adsorption experiments were carried out per the selected model with a pH range and WSAC dosage. The maximum removal of Cr^{2+} metal ions was 54.53% for WSAC at pH six and WSAC dosage of 0.6 g/l (Figure 7).

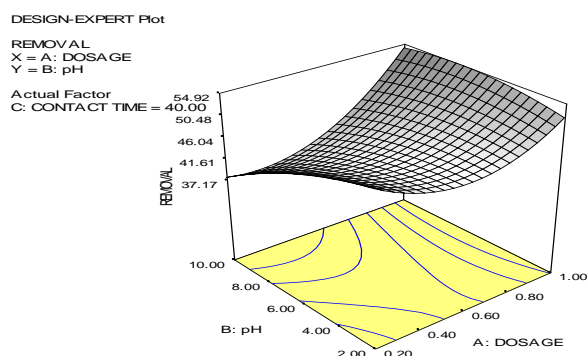


Figure 7 – A-3D interaction plot of the removal of Cr^{2+} using WSAC, the interaction of WSAC dosage and pH

Thus, with WSAC, adsorption takes place mainly in an acidic medium. Further, from the 3D graph obtained from the software, it is clear that the removal of Cr^{2+} increased at low pH values, afterwards, decreased with increased WSAC dosage.

Effect of contact time and dosage. The combined effect of WSAC dosage and contact time has been presented in Figure 4.8. The results show that the maximum removal was recorded at the 0.6 g/l WSAC dosage and contact time of 40 min. Further, from the 3D graph obtained from the software, it is clear that the removal of Cr^{2+} increased WSAC dosage and contact time and, afterwards, decreased with increased contact time.

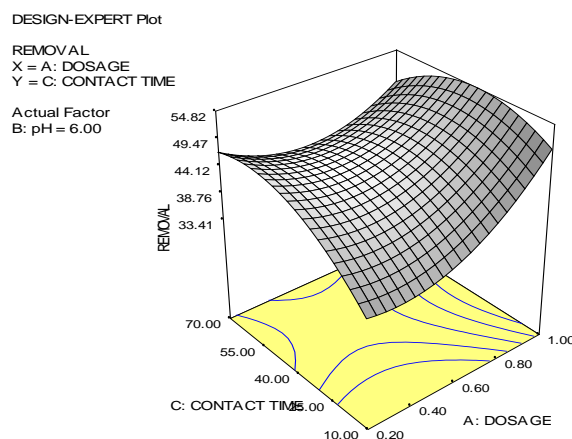


Figure 8 – A-3D interaction plot of the removal of Cr^{2+} using WSAC, the interaction of WSAC dosage and contact time

Effect of contact time and pH. The percentage removal of Cr^{2+} with WSAC powder was studied by a pre-selected range of time and pH values. The results are depicted in Figure 9. The results indicated that the maximum removal had occurred at a contact time of 40 min and pH of 6. Further, in the 3D graph obtained from the software, it is clear that the removal of Cr^{2+} at high contact time afterwards decreased and decreased with increased pH values.

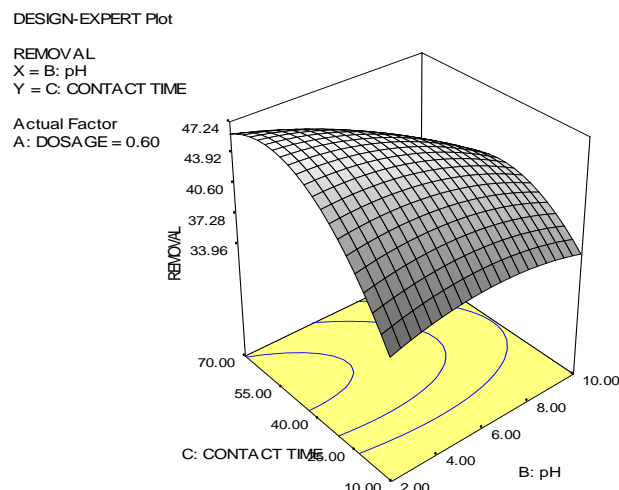


Figure 9 – A-3D interaction plot of the removal of Cr^{2+} using WSAC, the interaction of contact time and pH

CONCLUSIONS

A detailed batch experimental study was carried out for the removal of Cr^{2+} from wastewater by using Watermelon shell-activated carbon. The current study aimed to identify optimum process

conditions using response surface methodology for removing Cr²⁺ from textile effluent by WSAC as biosorbent. Response surface methodology using BBD proved a very effective and time-saving model for studying the influence of process parameters on response factors by significantly reducing the number of experiments and facilitating the optimum conditions. The Experimental values and the predicted values are in perfect match with an R² value of 0.978. This methodology could be successfully employed to study the importance of the test variables' individual, cumulative, and interactive effects in bio-sorption. The optimal removal of Cr was obtained at initial pH of 6.0 solution, WSAC dosage of 0.6 g/l and contact time of 40 min, resulting in 97.80% of the maximum predicted removal of Cr²⁺.

FTIR results confirmed the presence of different functional groups such as phenol, alcohol, carboxylic acid, alkanes, amines, amino acids, and aromatic alkyl halide in the Watermelon. Furthermore, the SEM image showed macro, meso, and micro-pore [26], which enhanced metal uptake.

Since the studied adsorption process in removing metal from textile effluent is efficient, further studies on the use of WSAC with high fixed carbon content should be carried out to investigate the effect on removal and compared with commercial activated carbon, which has been frequently employed in the industry. Also, further studies on the use of response surface methodology (RSM-BBD) should be employed for the adsorption of heavy metals.

REFERENCES

1. Tilley, E., Ulrich, L., Lüthi, C., Reymond, Ph., Zurbrügg, C. (2016). *Compendium of Sanitation Systems and Technologies* (2nd ed.). Duebendorf: Swiss Federal Institute of Aquatic Science and Technology.
2. Mwangi, I. W., Ngila, J. C., & Okonkwo, J. O. (2012). A comparative study of modified and unmodified maize tassels for removal of selected trace metals in contaminated water. *Toxicological & Environmental Chemistry*, 94(1), 20–39. doi: 10.1080/02772248.2011.638636
3. Yu, J.-G., Zhao, X.-H., Yu, L.-Y., Jiao, F.-P., Jiang, J.-H., & Chen, X.-Q. (2013). Removal, recovery and enrichment of metals from aqueous solutions using carbon nanotubes. *Journal of Radioanalytical and Nuclear Chemistry*, 299(3), 1155–1163. doi: 10.1007/s10967-013-2818-y
4. Monachese, M., Burton, J. P., & Reid, G. (2012). Bioremediation and Tolerance of Humans to Heavy Metals through Microbial Processes: a Potential Role for Probiotics? *Applied and Environmental Microbiology*, 78(18), 6397–6404. doi: 10.1128/aem.01665-12
5. Fenta, M. M. (2014). Heavy Metals Concentration in Effluents of Textile Industry, Tikur Wuha River and Milk of Cows Watering on this Water Source, Hawassa, Southern Ethiopia. *Research Journal of Environmental Sciences*, 8(8), 422–434. doi: 10.3923/rjes.2014.422.434
6. Kannan, V., Ramesh, R., & Sasikumar, C. (2005). Study on ground water characteristics and the effects of discharged effluents from textile units at Karur District. *Journal of environmental biology*, 26(2), 269–272.
7. Halimoon, N., & Yin, R. (2010). *Removal of Heavy Metals from Textile Wastewater using Zeolite*. Retrieved from https://www.researchgate.net/publication/289178886_Removal_of_Heavy_Metals_from_Textile_Wastewater_using_Zeolite
8. Mathur, N., Bhatnagar, P., & Bakre, P. (2005). Assessing mutagenicity of textile dyes from Pali (Rajasthan) using ames bioassay. *Applied Ecology and Environmental Research*, 4(1), 111–118.
9. WHO. (2013). *Lead poisoning and health*. Retrieved June 1, 2022, from <https://www.who.int/news-room/fact-sheets/detail/lead-poisoning-and-health>
10. Lingamdinne, L. P., Koduru, J. R., Jyothi, R. K., Chang, Y.-Y., & Yang, J.-K. (2015). Factors affect on bioremediation of Co(II) and Pb(II) onto Lonicera japonica flowers powder. *Desalination and Water Treatment*, 57(28), 13066–13080. doi: 10.1080/19443994.2015.1055813

11. Fatima, T., Nadeem, R., Masood, A., Saeed, R., & Ashraf, M. (2013). Sorption of lead by chemically modified rice bran. *International Journal of Environmental Science and Technology*, 10(6), 1255–1264. doi: [10.1007/s13762-013-0228-x](https://doi.org/10.1007/s13762-013-0228-x)
12. Mihajlović, M. T., Lazarević, S. S., Janković-Častvan, I. M., Kovač, J., Jokić, B. M., Janačković, D. T., & Petrović, R. D. (2014). Kinetics, thermodynamics, and structural investigations on the removal of Pb²⁺, Cd²⁺, and Zn²⁺ from multicomponent solutions onto natural and Fe(III)-modified zeolites. *Clean Technologies and Environmental Policy*, 17(2), 407–419. doi: [10.1007/s10098-014-0794-8](https://doi.org/10.1007/s10098-014-0794-8)
13. Wang, J., & Chen, C. (2009). Biosorbents for heavy metals removal and their future. *Biotechnology Advances*, 27(2), 195–226. doi: [10.1016/j.biotechadv.2008.11.002](https://doi.org/10.1016/j.biotechadv.2008.11.002)
14. Malik, R., Ramteke, D. S., Wate, S. R. (2006). Physico-chemical and surface characterization of adsorbent prepared from groundnut shell by ZnCl₂ activation and its ability to adsorb colour. *Indian Journal of Chemical Technology*, 13(4), 319–328.
15. Gavrilescu, M. (2004). Removal of Heavy Metals from the Environment by Biosorption. *Engineering in Life Sciences*, 4(3), 219–232. doi: [10.1002/elsc.200420026](https://doi.org/10.1002/elsc.200420026)
16. Olorundare, O. F., Krause, R. W. M., Okonkwo, J. O., & Mamba, B. B. (2012). Potential application of activated carbon from maize tassel for the removal of heavy metals in water. *Physics and Chemistry of the Earth, Parts A/B/C*, 50–52, 104–110. doi: [10.1016/j.pce.2012.06.001](https://doi.org/10.1016/j.pce.2012.06.001)
17. Moyo, M., & Chikazaza, L. (2013). Bioremediation of Lead(II) from Polluted Wastewaters Employing Sulphuric Acid Treated Maize Tassel Biomass. *American Journal of Analytical Chemistry*, 04(12), 689–695. doi: [10.4236/ajac.2013.412083](https://doi.org/10.4236/ajac.2013.412083)
18. Patil, B. S., Jayaprakasha, G. K., Chidambara Murthy, K. N., & Vikram, A. (2009). Bioactive Compounds: Historical Perspectives, Opportunities, and Challenges. *Journal of Agricultural and Food Chemistry*, 57(18), 8142–8160. doi: [10.1021/jf9000132](https://doi.org/10.1021/jf9000132)
19. Reddy, L. V., Reddy, Y. H. K., Reddy, L. P. A., & Reddy, O. V. S. (2008). Wine production by novel yeast biocatalyst prepared by immobilization on watermelon (*Citrullus vulgaris*) rind pieces and characterization of volatile compounds. *Process Biochemistry*, 43(7), 748–752. doi: [10.1016/j.procbio.2008.02.020](https://doi.org/10.1016/j.procbio.2008.02.020)
20. Mort, A., Zheng, Y., Qiu, F., Nimtz, M., & Bell-Eunice, G. (2008). Structure of xylogalacturonan fragments from watermelon cell-wall pectin. Endopolygalacturonase can accommodate a xylosyl residue on the galacturonic acid just following the hydrolysis site. *Carbohydrate Research*, 343(7), 1212–1221. doi: [10.1016/j.carres.2008.03.021](https://doi.org/10.1016/j.carres.2008.03.021)
21. Idris, S., Iyaka, Y. A., Ndamitso, M. M., Mohammed, E. B., & Umar, M. T. (2012). Evaluation of Kinetic Models of Copper and Lead Uptake from Dye Wastewater by Activated Pride of Barbados Shell. *American Journal of Chemistry*, 1(2), 47–51. doi: [10.5923/j.chemistry.20110102.10](https://doi.org/10.5923/j.chemistry.20110102.10)
22. Ye, J., Zhang, P., Hoffmann, E., Zeng, G., Tang, Y., Dresely, J., & Liu, Y. (2014). Comparison of Response Surface Methodology and Artificial Neural Network in Optimization and Prediction of Acid Activation of Bauxsol for Phosphorus Adsorption. *Water, Air, & Soil Pollution*, 225(12). doi: [10.1007/s11270-014-2225-1](https://doi.org/10.1007/s11270-014-2225-1)
23. Kiran, B., Kaushik, A., & Kaushik, C. P. (2007). Response surface methodological approach for optimizing removal of Cr (VI) from aqueous solution using immobilized cyanobacterium. *Chemical Engineering Journal*, 126(2–3), 147–153. doi: [10.1016/j.cej.2006.09.002](https://doi.org/10.1016/j.cej.2006.09.002)
24. Othman, N., Kueh, Y. S., Azizul-Rahman, F. H., & Hamdan, R. (2014). Watermelon Rind: A Potential Adsorbent for Zinc Removal. *Applied Mechanics and Materials*, 680, 146–149. doi: [10.4028/www.scientific.net/amm.680.146](https://doi.org/10.4028/www.scientific.net/amm.680.146)
25. Zarei, A., Bazrafshan, E., Khaksefidi, R., & Alizadeh, M. (2013). The Evaluation of Removal Efficiency of Phenol from Aqueous Solutions using Moringa Peregrina Tree Shell Ash. *Iranian Journal of Health Sciences*, 1(1), 65–74. doi: [10.18869/acadpub.jhs.1.1.65](https://doi.org/10.18869/acadpub.jhs.1.1.65)

26. Marsh, H., & Rodriguez-Reinoso, F. (2006). *Activated Carbon*. N. d. : Elsevier Science. doi: [10.1016/b978-0-08-044463-5.x5013-4](https://doi.org/10.1016/b978-0-08-044463-5.x5013-4)
27. Ketcha, J., Dina, D., Ngomo, H., & Ndi, N. (2012). *Preparation and Characterization of Activated Carbons Obtained from Maize Cobs by Zinc Chloride Activation*. *America Chemical Science Journal*, 2(4), 136-160.
28. Zarei, M., Niaei, A., Salari, D., & Khataee, A. (2010). Application of response surface methodology for optimization of peroxi-coagulation of textile dye solution using carbon nanotube–PTFE cathode. *Journal of Hazardous Materials*, 173(1–3), 544–551. doi: [10.1016/j.jhazmat.2009.08.120](https://doi.org/10.1016/j.jhazmat.2009.08.120)